

Sum Rate of MISO Neuro-spike Communication Channel with Constant Spiking Threshold

Hamideh Ramezani^{1,2}, *Student Member, IEEE*, Tooba Khan², *Student Member, IEEE* and Ozgur B. Akan^{1,2}, *Fellow, IEEE*

Abstract—Communication among neurons, known as neuro-spike communication, is the most promising technique for realization of a bio-inspired nanoscale communication paradigm to achieve biocompatible nanonetworks. In neuro-spike communication, the information, encoded into spike trains, is communicated to various brain regions through neuronal network. An output neuron needs to receive signal from multiple input neurons to generate a spike. Hence, in this paper, we aim to quantify the information transmitted through the multiple-input single-output (MISO) neuro-spike communication channel by taking into account models for axonal propagation, synaptic transmission and spike generation. Moreover, the spike generation and propagation in each neuron requires opening and closing of numerous ionic channels on the cell membrane, which consumes considerable amount of ATP molecules called metabolic energy. Thus, we evaluate how applying a constraint on available metabolic energy affects the maximum achievable mutual information of this system. To this aim, we derive a closed form equation for the sum rate of the MISO neuro-spike communication channel and analyze it under the metabolic cost constraints. Finally, we discuss the impacts of changes in number of pre-synaptic neurons on the achievable rate and quantify the trade-off between maximum achievable sum rate and the consumed metabolic energy.

Index Terms—Nanoscale communication, Neuro-spike communication, MISO Synaptic Channel, Channel capacity, Metabolic cost, Spike generation

I. INTRODUCTION

Realization of bio-inspired nanonetworks require biocompatible communication paradigm. Thus, molecular communication [1], being the part of natural processes, is regarded as the most promising technique for this purpose. To investigate molecular communication in natural processes, we focus on communication among neurons, called neuro-spike communication, building block of a highly evolved and efficient molecular communication based nanonetwork [2].

Information theoretical analysis of neuro-spike communication is done in various studies [3]–[9] using different channel models. In [3], Hodgkin-Huxley (HH) model is used to calculate information capacity. In [4], the information transfer rate for single-input single-output (SISO) system is calculated

using a probabilistic model, which is extended in [5] to find the information rate in a SISO model with multiple synaptic terminals between two neurons. In [6], the upper bound of the capacity for a SISO synaptic communication is derived using Bernoulli distribution to model diffusion process.

Cortical neurons need to receive stimulation from several input neurons to fire an action potential [10]. Moreover, neurospike communication is a communication paradigm for nanonetworks, where nanomachines can receive information from several inputs. Hence, the information transfer rate for MISO neuro-spike communication is derived in [7]. However, all these studies ignore the impact of synaptic geometry, diffusion of neurotransmitters, their clearance from the synaptic cleft and the spike generation. Recently, realistic communication models are used in [8], [9] to study the capacity of vesicle release process and synaptic transmission, respectively. However, the performance of the overall neuro-spike communication channel is not considered in these studies.

The brain consumes dramatically lower power compared to man-made computers [11]. Moreover, as shown in [12], the properties of thalamic relay synapses are set to maximize information transmitted per used ATP molecule instead of information transmitted per second. The information capacity of the H-H model and an empirical neuronal signaling model is investigated under metabolic cost constraint in [13] and [14], respectively. It is concluded that the capacity increases as the upper bound on the consumed metabolic energy is relaxed. Therefore, including metabolic constraints in the model is inevitable to accurately evaluate the rate of information transmission over neuro-spike communication channel.

In this paper, we consider the MISO neuro-spike communication among hippocampal pyramidal neurons. Thus, the input of the communication channel is spike trains of all pre-synaptic terminals and the output is the fired spikes in post-synaptic neuron. We consider realistic communication models for different processes involved in this communication such as synaptic geometry, diffusion of neurotransmitters, and their re-uptake by pre-synaptic terminal. Using this communication model and considering all possible variations in biophysical parameters of pre- and post-synaptic neurons, we analyze the maximum achievable rate of information transmission over our model subject to the metabolic cost constraints and derive a general closed form equation for the sum rate of MISO neuro-spike communication channel. Moreover, to get an insight on the impact of the number of pre-synaptic neurons on the performance of MISO channel while reducing the complexity of the system, we consider the same biophysical parameters for

¹H. Ramezani and O. B. Akan are with the Internet of Everything (IoE) Group, Electrical Engineering Division, Department of Engineering, University of Cambridge, Cambridge CB3 0FA, UK

²H. Ramezani, T. Khan and O. B. Akan are with the Next-generation and Wireless Communications Laboratory (NWCL), Department of Electrical and Electronics Engineering, Koç University, Istanbul 34450, Turkey
Emails: hr404@cam.ac.uk, tkhan15@ku.edu.tr, oba21@cam.ac.uk

This work was supported in part by ERC Project MINERVA under grant ERC-2013-CoG 616922 and by TÜBİTAK graduate scholarship program under grant BİDEB-2215.

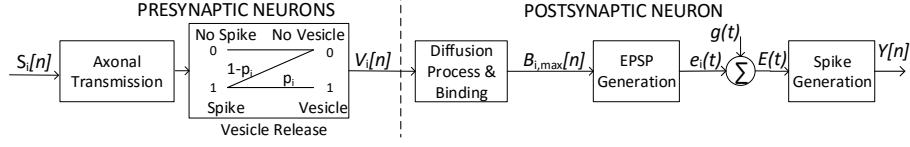


Fig. 1. Block diagram of the communication channel between i th pre-synaptic neuron and the output neuron.

all pre-synaptic neurons and derive a closed form equation for the sum rate of the channel, which is later used in simulations. Finally, we study how the performance of MISO channel is influenced by changes in the biophysical parameters of the channel, which can happen as a result of different diseases.

The rest of the paper is organized as follows. In Section II, we describe the MISO synaptic channel model. In Section III, we formulate the sum rate of MISO neuro-spike communication channel under metabolic cost constraints. In Section VI, we present and discuss simulation results. Finally, we conclude the paper in Section V.

II. MODEL DESCRIPTION

In this section, we define processes included in the MISO neuro-spike communication channel as shown in Fig. 1.

A. Axonal Transmission

Linear-Nonlinear-Poisson (LNP) model is one of the neural coding models used to encode external stimulus into spiking rate [7]. According to LNP model, the resulting spike train follows Poisson random distribution. Thus, in this paper, pre-synaptic neurons generate spike trains, $S_i(t)$, following Poisson processes with rate λ_i [8], where $i \in [1, M]$ and M is the number of pre-synaptic inputs. After firing a spike in a pre-synaptic neuron, another spike cannot be generated for a short time called refractory period [10]. Hence, we can divide time into windows of equal duration Δt , where Δt is small enough to contain only one spike. Thus, a discrete time random variable $S_i[n]$ is defined to indicate the occurrence of a spike in n th time step with the probability $P\{S_i[n] = 1\} = 1 - \exp(-\lambda_i \Delta t)$.

Each spike is then transmitted to pre-synaptic terminals through axon. Although the spike shape may change during axonal transmission [15], more experimental data is needed to accurately model functionality of axon [16]. Hence, we consider the axon as an ideal filter, which is a fairly accurate model for hippocampal pyramidal neurons since their axonal transmission is highly reliable due to the existence of myelin sheaths and Node of Ranvier [17]. Thus, the output of axonal transmission in i th pre-synaptic neuron is $S_i[n]$.

B. Vesicle Release Process

At least two pools of vesicles exist in each pre-synaptic terminal depending on their distance from the membrane and their mobility [10]. The pool of vesicles that are ready for release on the arrival of spike is called readily releasable pool (RRP) with size N_i , where $i \in [1, M]$. Similar to [7], instantaneous replenishment of RRP after each release is considered in this paper, i.e., N_i remains constant over time.

The rate at which vesicles are fused with the membrane of i th pre-synaptic terminal in n th window is $\alpha_i = 0.06\sqrt{N_i}$ [18]. Then, the probability of vesicle release during n th window, i.e., $V_i[n] = 1$, given spike arrival is [7]

$$P\{V_i[n] = 1 | S_i[n] = 1\} = 1 - \exp(-N_i \alpha_i) \triangleq P_i.$$

Since the spontaneous release probability is very low in hippocampal neurons [19], we ignore it in this study, thus, $P\{V_i[n] = 1 | S_i[n] = 0\} = 0$.

C. Diffusion Process

Once a vesicle is released, neurotransmitters diffuse through the synaptic cleft to reach post-synaptic density (PSD) that contains receptors. As defined in [20], we consider a rectangular synaptic cleft for i th synapse with height H_i and a square shaped PSD with side length L_i on post-synaptic membrane. In [20], the pre- and post-synaptic membranes are assumed to have infinite dimension. Then, the expected value of concentration of neurotransmitters in the synaptic cleft from i th pre-synaptic input at time t , $C_i(x, y, z, t)$, is given as,

$$C_i(x, y, z, t) = \frac{T_0}{(\sqrt{4\pi D_c t})^3} e^{\frac{-(x^2 - y^2)}{4D_c t}} \left\{ \sum_{k=-\infty}^{-1} (2 - P_{i,u})(1 - P_{i,u})^{-(k+1)} e^{\frac{-(z - (2k+1)H_i)^2}{4D_c t}} + \sum_{k=0}^{\infty} (2 - P_{i,u})(1 - P_{i,u})^k e^{\frac{-(z - (2k+1)H_i)^2}{4D_c t}} \right\}, \quad (1)$$

where T_0 is the number of neurotransmitters in a vesicle, $P_{i,u}$ is the uptake probability in i th synapse and its unit is uptake per hit, D_c is diffusion coefficient, $0 \leq t \leq \Delta t$ and $(x, y, z) \in \mathbb{R}^2 \times [0, H_i]$.

The neurotransmitters that reach post-synaptic terminal bind to the receptors residing on the PSD. These receptors are assumed to be uniformly distributed on the PSD and a small effective volume, i.e., $v_{i,r}$, is considered around r th receptor located in i th synapse such that the neurotransmitters that are inside this volume are likely to bind with the receptor [20]. The expected concentration of neurotransmitters inside $v_{i,r}$, i.e., $C_{v_{i,r}}(t)$, is calculated in [20] as

$$C_{v_{i,r}}(t) \approx \frac{\overline{T_{i,r}(t)}}{|v_{i,r}|}$$

where $T_{i,r}(t)$ is the number of neurotransmitters found inside $v_{i,r}$ at time t and $|v_{i,r}|$ is the size of the effective volume. As shown in [20], $T_{i,r}(t)$ can be modeled by a binomial random variable, having expected value $\overline{T_{i,r}(t)} = T_i(t)P_{i,r}(t)$. Here, $T_i(t) \leq T_0$ is the expected total number of unbound neurotransmitters in the i th synaptic cleft at time t and $P_{i,r}(t)$

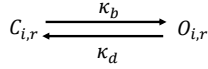


Fig. 2. Kinetic scheme of AMPA receptors.

is the probability of finding a released neurotransmitter inside $v_{i,r}$ at time t . This probability is calculated in [20] as

$$P_{i,r}(t) = \iiint_{v_{i,r}} C_i(x, y, z, t) dx dy dz,$$

where C_i is given by (1) with $T_0 = 1$, $i \in [1, M]$, $r \in [1, R_0]$ and R_0 is the total number of receptors on a PSD.

D. Neurotransmitter-Receptor Binding

Binding of the released neurotransmitters to receptors located on the post-synaptic terminal can either (i) decrease the membrane potential of the output neuron, happening in inhibitory synapses, or (ii) increase it, occurring in excitatory synapses [10]. The focus of this study is on hippocampal pyramidal neurons, where excitatory synapses are the most abundant type [10] and the major receptors are AMPA and NMDA. Since NMDA receptors contribute in synaptic plasticity, which is not addressed in this paper, we only consider the excitatory post-synaptic potential (EPSP) generated by AMPA receptors. Moreover, we utilize the kinetic model demonstrated in Fig. 2 for binding of neurotransmitters to AMPA receptors since it provides a good approximation for the time course and the dynamic behavior of synaptic currents [21].

In the Kinetic model shown in Fig. 2, κ_b and κ_d are binding and dissociation rates for AMPA receptors, respectively. Each receptor r , $r \in [1, R_0]$, located in the synaptic terminal made by i th pre-synaptic neuron can have two states, (i) close state, $C_{i,r}$, where the receptor is available to bind to a neurotransmitter, and (ii) open state, $O_{i,r}$, where the receptor is bound to a neurotransmitter and cannot bind to another one before unbinding from the current one. The expected concentration of neurotransmitters near receptor, i.e., $C_{v_{i,r}}(t)$, controls the probability of these states as given below.

$$\begin{aligned} \frac{dC_{i,r}(t)}{dt} &= -\kappa_b C_{i,r}(t) C_{v_{i,r}}(t) + \kappa_d O_{i,r}(t), \\ C_{i,r}(t) + O_{i,r}(t) &= 1, \end{aligned}$$

where $(n-1)\Delta t \leq t \leq n\Delta t$. $O_{i,r}(t)$ and $C_{i,r}(t)$ represent the opening and closing probabilities of a receptor, respectively, that depend on both time and the position of receptors.

E. Post-synaptic Potential at Each Synapse

The receptors allow the influx of ions to the post-synaptic neuron after entering the open state. This changes the post-synaptic membrane potential, which is modeled as

$$e_i(t) = \begin{cases} h_i \frac{t}{t_p} \exp(1 - \frac{t}{t_p}), & t \geq 0 \\ 0, & t < 0 \end{cases} \quad (2)$$

where h_i is the peak EPSP amplitude contributed by i th synapse and t_p is time to reach the peak [7].

Considering the vesicle release in n th time step, the contribution of i th synapse in the post-synaptic membrane potential can be written as $e_i(t - t_n) = B_{i,max}[n] h_p(t - t_n)$, where $h_p(t) = h_p \frac{t}{t_p} \exp(1 - \frac{t}{t_p})$, h_p is the maximum membrane potential contributed by each receptor, $B_{i,max}[n]$ is the maximum number of bound receptors, and t_n is the beginning of n th time step. After binding to a neurotransmitter, receptors stay in open state until EPSP reaches its maximum value [20]. Hence, the maximum of $O_{i,r}(t)$ for $(n-1)\Delta t \leq t < n\Delta t$ and all receptors in i th synapse can be used to derive $B_{i,max}[n]$. Consider $O_{i,r}[n] = \max_{(n-1)\Delta t \leq t < n\Delta t} (O_{i,r}(t))$ and define the variable $x_{i,r}[n]$ as follows.

$$x_{i,r}[n] = \begin{cases} 0, & 1 - O_{i,r}[n] \\ 1, & O_{i,r}[n] \end{cases}$$

Then, $\sum_{r=1}^{R_0} x_{i,r}[n]$ shows the maximum number of open receptors during n th time step. Hence, the probability of having j open receptors upon vesicle release can be derived as $P\{B_{i,max}[n] = j | V_i[n] = 1\} = P\{\sum_{r=1}^{R_0} x_{i,r}[n] = j\}$. Thus, this probability can be modeled by Poisson Binomial distribution with mean, $\mu_i[n] = \sum_{r=1}^{R_0} O_{i,r}[n]$, and variance, $\sigma_i[n]^2 = \sum_{r=1}^{R_0} O_{i,r}[n](1 - O_{i,r}[n])$ [22].

F. Spike Generation

The EPSP generated by each synapse is integrated at soma to derive the membrane potential of post-synaptic neuron as

$$E(t) = e_0 + \sum_{i=1}^M \sum_{t_n \leq t, \forall n} V_i[n] e_i(t - t_n) + g(t), \quad (3)$$

where e_0 is the resting membrane potential, t_n is the beginning of n th time slot and $g(t)$ is the noise in post-synaptic membrane voltage. Different noise sources such as thermal noise, leakage from ionic channels and synaptic noise can corrupt the membrane voltage of the output neuron. Synaptic noise is due to the multiple access to the synapse, which results in the reception of residual neurotransmitters released at thousands of other synapses in previous time steps. Since signal of different neurons has the same random structure and due to the central limit theorem, the probability density function of the post-synaptic noise converges to a Gaussian process, whose mean and variance are considered as zero and σ_n^2 , respectively [7].

A spike occurs in the post-synaptic neuron when the changes in the post-synaptic membrane potential is strong enough. To model this process, we consider a fixed spiking threshold, θ_0 . When $E(t) \geq \theta_0$ a spike is fired by post-synaptic neuron, i.e., $Y[n] = 1$, and the post-synaptic membrane potential is set to the resting membrane potential, i.e., e_0 . While the spike generation threshold can change according to previous stimulations of the post-synaptic neuron [23], considering a fix spiking threshold provides the chance to analyze the impact of spike generation on the performance of neuro-spike communication for the first time in the literature.

III. SUM RATE ANALYSIS WITH METABOLIC ENERGY CONSTRAINT ON NEURONAL SIGNALING

For analyzing the achievable rate of information transmission over our model, we use basic definitions from information theory. The input and output of our model are the spike train, $S_i[n]$ and the generated spikes at output, $Y[n]$, respectively. Thus, the mutual information of the channel is derived as

$$I(S^M[n]; Y[n]) = H(Y[n]) - H(Y[n]|S^M[n]), \quad (4)$$

where $S^M[n] = \{S_1[n], S_2[n], \dots, S_M[n]\}$. While within each time step the generated EPSP at output neuron, i.e., $E(t)$, changes with time, the channel model shown in Fig. 1 does not vary from one time step to another time step. Moreover, the probability distribution of spike generation at inputs does not change with time. Furthermore, we study the situation where the width of $e_i(t)$ given in (2) is smaller than discretization time step, Δt . Hence, the channel transmission probability, i.e., $P\{Y[n]|S^M[n]\}$, and the probability of spike generation at the output neuron, i.e., $P\{Y[n] = 1\}$, thus, the mutual information among input and output of the channel, i.e., $I(S^M[n]; Y[n])$, does not depend on the time step.

The capacity region of the multiple-access channel is the maximum mutual information, maximized over all input distribution, $p(S^M[n])$. Since in real scenario, spike trains from different inputs are independently generated by $S_i[n] \sim Poiss(\lambda_i)$, the mutual information can be maximized over λ_i for $\forall i$ to study the maximum achievable rate of information transmission over this channel. Defining R_i as the achievable rate for i th pre-synaptic neuron, the upper bound on the achievable sum rate of the MISO channel is derived as

$$\sum_{i=1}^M R_i \leq \max_{\forall i, \lambda_i} I(S^M[n]; Y[n]) \triangleq C.$$

Note that C is the maximum rate at which we can send information with a vanishingly low probability of error over this channel using the Poisson distribution for spike generation at input neurons. However, in physical systems, this sum rate is limited by some physical, chemical or biological factors. In neuronal networks, one of the significant limiting factors is the energy being consumed for neural activities, w , in terms of number of ATP molecules, called metabolic energy. For the MISO channel with M pre-synaptic and one post-synaptic neuron, the metabolic energy associated with each input-output pair in n th time window is calculated as [24],

$$w(S^M[n], Y[n]) = (M + 1)\beta\Delta t + \kappa(Y[n] + \sum_{i=1}^M S_i[n]),$$

where $\beta = 0.342 \times 10^9$ ATP molecules per second is required to maintain resting potential and $\kappa = 0.71 \times 10^9$ ATP molecules is required to generate a single spike [13]. Thus, the average metabolic energy consumed in n th time step is

$$w_p[n] = \sum_{S^M, Y} w(S^M[n], Y[n])p(S^M[n], Y[n]). \quad (5)$$

Considering that average consumed metabolic energy in n th time step must be bound to W ATP molecules, the maximum

achievable transmission rate of the MISO channel under the metabolic cost constraints is given below.

$$C(W) = \max_{\forall i, \lambda_i: w_p[n] \leq W} I(S^M[n]; Y[n]). \quad (6)$$

To derive the mutual information between input, $S^M[n]$, and output, $Y[n]$, of the MISO neuro-spike communication channel, we calculate $p\{Y[n]\}$ and $p\{Y[n]|S^M[n]\}$ in this section. The membrane potential of the post-synaptic neuron before spike generation is given by (3). Since, the time is discretized, we consider that the spikes occur at the beginning of each time slot. Thus, by selecting the Δt greater than or equal to the duration of Action Potential, there is no overlap among the EPSP in consecutive time-steps. Hence, $P\{Y[n] = 1\}$ can be derived as,

$$\begin{aligned} P\{Y[n] = 1\} &= P\{E(t) > \theta_0\} \\ &= P\{e_0 + \sum_{i=1}^M V_i[n]B_{i,\max}[n]h_p(t - t_n) + g(t) > \theta_0\}. \end{aligned}$$

By conditioning over $V^M[n] = \{V_1[n], V_2[n], \dots, V_M[n]\}$ and $B^M[n] = \{B_{1,\max}[n], B_{2,\max}[n], \dots, B_{M,\max}[n]\}$, the $P\{Y[n] = 1\}$ can be derived as

$$\begin{aligned} P\{Y[n] = 1\} &= \sum_{\underline{v}, \underline{b}} P\{B^M = \underline{b}, V^M = \underline{v}\} \\ &P\left\{g(t) > \theta_0 - e_0 - \sum_{i=1}^M v_i b_i h_p(t - t_n) \mid B^M = \underline{b}, V^M = \underline{v}\right\}, \end{aligned}$$

where \underline{v} and \underline{b} are $1 \times M$ arrays with i th element $v_i \in \{0, 1\}$ and $b_i \in [0, R_0]$, respectively. The Gaussian noise is independent from vesicle release process and the neurotransmitter-receptor binding, thus, we get

$$\begin{aligned} P\{Y[n] = 1\} &= \sum_{\underline{v}, \underline{b}} P\{B^M = \underline{b}, V^M = \underline{v}\} \\ &P\left\{g(t) > \theta_0 - e_0 - \sum_{i=1}^M v_i b_i h_p(t - t_n)\right\}. \end{aligned} \quad (7)$$

In the spike generation process, $Y[n] = 1$ if $g(t) > \theta_0 - e_0 - \sum_{i=1}^M v_i b_i h_p(t - t_n)$ at any instant of time within $t_n < t < t_n + \Delta t$. Moreover, $g(t)$ is Gaussian, thus, $P\{g(t) > g_0\}$ increases as g_0 decreases. Therefore, by achieving the minimum of $\theta_0 - e_0 - \sum_{i=1}^M v_i b_i h_p(t - t_n)$ that happens when $h_p(t - t_n)$ is maximum, (7) can be simplified to,

$$\begin{aligned} P\{Y[n] = 1\} &= \sum_{\underline{v}, \underline{b}} P\{B^M = \underline{b}, V^M = \underline{v}\} \\ &P\left\{g(t_n + t_p) > \theta_0 - e_0 - \sum_{i=1}^M v_i b_i h_p\right\}, \end{aligned}$$

where

$$\begin{aligned} P\{B^M = \underline{b}, V^M = \underline{v}\} &= P\{B^M = \underline{b} \mid V^M = \underline{v}\} P\{V^M = \underline{v}\} \\ &= \left(\prod_{i=1}^M P\{B_{i,\max}[n] = b_i \mid V_i[n] = v_i\} \right) P\{V^M = \underline{v}\}. \end{aligned}$$

Here, $P\{B_{i,\max}[n] = 0|V_i[n] = 0\} = 1$ and $P\{B_{i,\max}[n] = b_i|V_i[n] = 1\}$ is given by Poisson Binomial distribution. Moreover,

$$P\{V^M = \underline{v}\} = \sum_{\underline{s}} P\{V^M = \underline{v}|S^M = \underline{s}\} P\{S^M = \underline{s}\} \\ = \sum_{\underline{s}} \left(\prod_{i=1}^M P\{V_i[n] = v_i|S_i[n] = s_i\} \right) P\{S^M = \underline{s}\}$$

where \underline{s} is a $1 \times M$ array with i th element $s_i \in \{0, 1\}$ and $P\{S^M = \underline{s}\}$ depends on the correlation among the spike trains of different inputs. Whereas, $P\{V_i[n] = v_i|S_i[n] = s_i\}$ is defined in Section II-B. According to the law of total probability $P\{Y[n] = 1\}$ can be written as

$$P\{Y[n] = 1\} = \sum_{\underline{s}} P\{Y[n] = 1|S^M[n] = \underline{s}\} P\{S^M = \underline{s}\}$$

and the conditional probability $P\{Y[n]|S^M[n]\}$ is derived as

$$P\{Y[n] = 1|S^M[n] = \underline{s}\} = \\ \sum_{\underline{b}, \underline{v}} \left(P\left\{g(t_n + t_p) > \theta_0 - e_0 - \sum_{i=1}^M v_i b_i h_p\right\} \right. \\ \left. \prod_{i=1}^M P\{B_{i,\max}[n] = b_i|V_i[n] = v_i\} \right. \\ \left. \prod_{i=1}^M P\{V_i[n] = v_i|S_i[n] = s_i\} \right).$$

In this section, we derived the closed form equation for sum rate of MISO neuro-spike communication channel considering a detailed channel model. To simulate derived equations for $P\{Y[n] = 1\}$ and $P\{Y[n] = 1|S^M[n] = \underline{s}\}$, all possible combinations of \underline{b} , \underline{v} and \underline{s} must be considered. Since $b_i \in [0, R_0]$ and $v_i, s_i \in [0, 1]$, the number of these combinations is $R_0^M \times 2^M \times 2^M$. Hence, while derived formulas can be used to study the performance of neuro-spike communication for small values of M , the complexity of simulating this model grows exponentially with the number of pre-synaptic neurons, i.e., M , as a result of complexity of neuro-spike communication. Hence, to provide a framework for analyzing impacts of increasing number of pre-synaptic terminals and variations in biophysical parameters of the channel when M is high, we consider a simplified scenario in next section. We assume that all pre-synaptic neurons have the same biophysical parameters and derive another closed form equation for mutual information among input and output of the channel under this situation. The following analysis also gives insights on the performance of artificial nanonetworks, where identical nanomachines communicate with each other using the communication paradigm inspired from synaptic transmission.

A. Pre-synaptic Neurons with Same Synaptic Structure

Here, we assume that biophysical parameters of all input neurons and their synapse to the output neuron are the same, i.e., for $\forall i_1, i_2 \in [1, M]$ and $\forall r$ following equations hold.

$$\begin{aligned} N_{i_1} &= N_{i_2} & P_{i_1} &= P_{i_2} & H_{i_1} &= H_{i_2} \\ L_{i_1} &= L_{i_2} & P_{i_1, u} &= P_{i_2, u} & v_{i_1, r} &= v_{i_2, r} \end{aligned}$$

Hence, the number of spikes arrive at input determines number of released vesicles. Consequently, the number of bound neurotransmitters to the receptors and the generated post-synaptic potential only depend on the number of arrived spikes at input. In other words, knowing which pre-synaptic neuron is transmitting a spike does not affect the output. Hence, (4) can be written as follows.

$$I(S^M[n]; Y[n]) = H(Y[n]) - H(Y[n]|\sum_{i=1}^M S_i[n] = s_t). \quad (8)$$

In the following, we derive $P\{Y[n] = 1\}$ and $P\{Y[n] = 1|\sum_{i=1}^M S_i[n] = s_t\}$. By conditioning over number of bound neurotransmitter, $P\{Y[n] = 1\}$ can be written as

$$P\{Y[n] = 1\} = \sum_{b_t} P\left\{\sum_{i=1}^M V_i[n] B_{i,\max}[n] = b_t\right\} \\ P\left\{g(t) > \theta_0 - e_0 - b_t h_p\right\},$$

where $b_t \in [0, MR_0]$ shows total number of bound receptors in all synapses to the post-synaptic terminal. Since all pre-synaptic neurons and their synapse to the post-synaptic neuron are identical, number of released vesicles is the important parameter in finding b_t and the place of release is not important. Hence, without loss of generality, we assume that in case of j release, the vesicle release is occurred from 1st to j th synapse. Thus, $P\{\sum_{i=1}^M V_i[n] B_{i,\max}[n] = b_t\}$ can be written as

$$P\left\{\sum_{i=1}^M V_i[n] B_{i,\max}[n] = b_t\right\} = \\ \sum_{j=1}^M P\left\{\sum_{i=1}^j B_{i,\max} = b_t \mid \sum_{i=1}^M V_i[n] = j\right\} P\left\{\sum_{i=1}^M V_i[n] = j\right\} \\ + P\left\{\sum_{i=1}^M V_i[n] B_{i,\max}[n] = b_t \mid \sum_{i=1}^M V_i[n] = 0\right\} P\left\{\sum_{i=1}^M V_i[n] = 0\right\}$$

where $P\{\sum_{i=1}^M V_i[n] B_{i,\max}[n] = 0 \mid \sum_{i=1}^M V_i[n] = 0\} = 1$. Considering $j \geq 1$ released vesicles, the total number of bound receptors, b_t , cannot be greater than jR_0 . Hence, for $b_t > jR_0$,

$$P\left\{\sum_{i=1}^j B_{i,\max} = b_t \mid \sum_{i=1}^M v_i = j\right\} = 0$$

and for $b_t \leq jR_0$,

$$P\left\{\sum_{i=1}^j B_{i,\max} = b_t \mid \sum_{i=1}^M v_i = j\right\} = P\left\{\sum_{i=1}^j \sum_{r=1}^{R_0} x_{i,r}[n] = b_t\right\},$$

which can be modeled by Poisson Binomial distribution with mean, $\mu_t[n]$, and variance, $\sigma_t[n]^2$, as shown in [22],

$$\mu_t[n] = \sum_{i=1}^j \sum_{r=1}^{R_0} O_{i,r}[n], \quad (9)$$

$$\sigma_t[n]^2 = \sum_{i=1}^j \sum_{r=1}^{R_0} O_{i,r}[n](1 - O_{i,r}[n]). \quad (10)$$

Next step is deriving $P\{\sum_{i=1}^M V_i[n] = j\}$. The number of released vesicles depends on the total number of spikes arrived in different pre-synaptic terminals in n th time window. Thus,

$$P\left\{\sum_{i=1}^M V_i[n] = j\right\} = \sum_{s_t} P\left\{\sum_{i=1}^M V_i[n] = j \mid \sum_{i=1}^M S_i[n] = s_t\right\} P\left\{\sum_{i=1}^M S_i[n] = s_t\right\}.$$

Since we ignore the probability of spontaneous release in this study, number of released vesicles to all synapses, i.e., j , cannot be greater than total number of arrived spikes to all pre-synaptic terminals, i.e., s_t . Hence, for $j > s_t$,

$$P\left\{\sum_{i=1}^M V_i[n] = j \mid \sum_{i=1}^M S_i[n] = s_t\right\} = 0$$

and for $j \leq s_t$,

$$P\left\{\sum_{i=1}^M V_i[n] = j \mid \sum_{i=1}^M S_i[n] = s_t\right\} = \binom{s_t}{j} P_i^j (1 - P_i)^{s_t - j}.$$

According to the law of total probability $P\{Y[n] = 1\}$ can be written as

$$P\{Y[n] = 1\} = \sum_{s_t=0}^M \left(P\{Y[n] = 1 \mid \sum_{i=1}^M S_i[n] = s_t\} P\left\{\sum_{i=1}^M S_i[n] = s_t\right\} \right)$$

and the conditional probability $p\{Y[n] \mid \sum_{i=1}^M S_i[n] = s_t\}$ is derived as

$$P\left\{Y[n] = 1 \mid \sum_{i=1}^M S_i[n] = s_t\right\} = \sum_{j=1}^{s_t} \sum_{b_t=0}^{jR_0} P\left\{g(t) > \theta_0 - e_0 - b_t h_p\right\} P\left\{\sum_{i=1}^j \sum_{r=1}^{R_0} x_{i,r}[n] = b_t\right\} \binom{s_t}{j} P_i^j (1 - P_i)^{s_t - j} + P\left\{g(t) > \theta_0 - e_0\right\} (1 - P_i)^{s_t}.$$

Note that the second term of this equation is derived for $j = 0$ and consequently $b_t = 0$.

Considering spike arrival in different pre-synaptic neurons as independent, the probability of having s_t spikes in all pre-synaptic terminals, i.e., $P\{\sum_{i=1}^M S_i[n] = s_t\}$ is derived based on Poisson-Binomial distribution with mean, μ_{st} , and, variance, σ_{st}^2 , given below.

$$\mu_{st} = \sum_{i=1}^M P\{S_i[n] = 1\}, \quad (11)$$

$$\sigma_{st}^2 = \sum_{i=1}^M P\{S_i[n] = 1\} (1 - P\{S_i[n] = 1\}).$$

Note that by using same spike rate for different pre-synaptic terminals, $P\{\sum_{i=1}^M S_i[n] = s_t\}$ can be derived based on Binomial distribution with mean, μ_{st} , and, variance, σ_{st}^2 .

TABLE I
SIMULATION PARAMETERS

Parameters	Symbols	Values
Time to reach peak of EPSP	t_p	220 μ s [20]
Size of RRP	N_i for $\forall i$	10 [25]
Resting potential	e_0	-65 mV
Spiking threshold	θ_0	-45 mV [26]
Noise standard deviation	σ_n	0.1 mV [7]
Neurotransmitters in a vesicle	T_0	300
Synaptic cleft height	H_i for $\forall i$	20 nm [27]
Diffusion coefficient	D_c	0.33 μ m ² /ms [28]
Side length of PSD	L_i for $\forall i$	0.4 μ m [20]
Receptor density	[AMPA]	500/ μ m ² [29]
Pre-synaptic re-uptake	$P_{i,u}$ for $\forall i$	10% [20]
Binding rate of AMPA	κ_b	$78 \times 10^6 \frac{1}{\text{Ms}}$ [30]
Dissociation rate of AMPA	κ_d	750 s^{-1} [30]
Effective volume	$ V_{i,r} $ for $\forall i, r$	$1 \times 1 \times 0.5 \text{ nm}^3$
Simulation time step	$\Delta\tau$	3.85 ns [20]
Time step and spike width	$\Delta t = \Delta t_s$	4 ms [8], [10]

IV. SIMULATION RESULTS AND DISCUSSION

In this section, we evaluate the sum rate of MISO neuro-spike communication channel by considering same characteristics for all pre-synaptic inputs given in Table I. Moreover, we consider that all pre-synaptic neurons use same spiking rate, i.e., $\lambda_i = \lambda$. Note that we utilize a smaller simulation time step, called $\Delta\tau$, within Δt to derive $O_{i,r}(t)$ [20]. Moreover, the peak EPSP amplitude contributed by i th synapse is calculated as $h_i = h_p B_{i,max}[n]$, where h_p is fixed such that $h_i = 1$ mV for parameters given in Table I [7]. Variations in parameters may lead to different values of h_i as $B_{i,max}[n]$ may change. Furthermore, t_p depends on synaptic parameters such as number of neurotransmitters in each vesicle, re-uptake probability, synaptic geometries, and offset in vesicle release site [20]. If these parameters change in a way that t_p increases, the shape of $e_i(t)$ widens, which can result in $e_i(t)$ that is wider than the discretization time step, Δt . In this case, the probability of spike generation at output, i.e., $P\{Y[n] = 1\}$, depends on released vesicles in previous time steps, thus the mutual information of the channel changes with time, which is not under the focus of this study. The results reported in this section give insight in the way neurons communicate and the performance of nanonetwork designed based on neuro-spike communication paradigm. Further studies are required to investigate impacts of selecting synaptic parameters that lead to bigger values of t_p on the performance of this communication channel.

A. Mutual Information

In this section, we evaluate impacts of changes in spiking rate, λ , and the number of inputs, M , on the mutual information between input and output of the channel, I .

To generate a spike in post-synaptic terminal, its membrane potential needs to increase from resting potential, i.e., $e_0 = -65$ mV, to spiking threshold, i.e., $\theta_0 = -45$ mV. Two factors are important in finding the average number

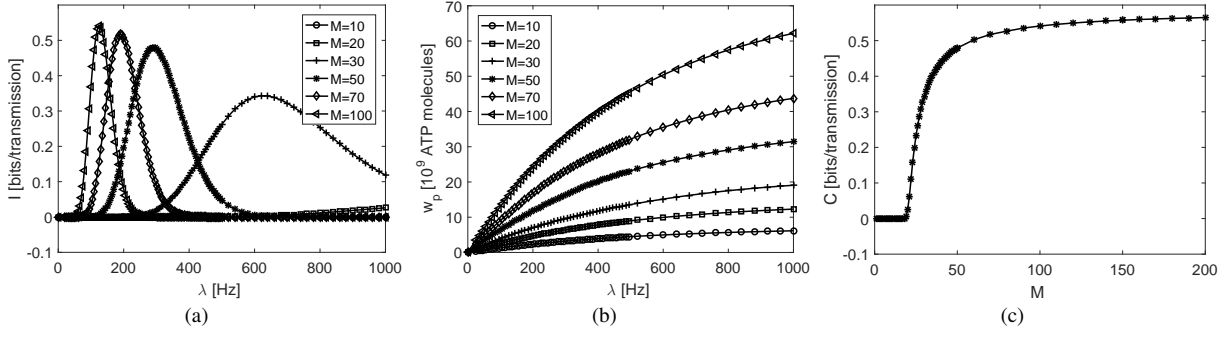


Fig. 3. (a) Mutual information, I , (b) average consumed metabolic energy, w_p , and (c) maximum achievable sum rate for different number of neurons, M .

of spikes needed at input to cause this required potential change (i) vesicle release probability after spike arrival to a pre-synaptic terminal, i.e., $P_i = 0.85$, and (ii) the average contribution of each pre-synaptic terminal in post-synaptic membrane potential after vesicle release, which is considered as $\overline{B_{i,max}[n]}h_p = 1\text{mV}$ same as [7]. Hence, on average, arrival of more than $\frac{\theta_0 - e_0}{\overline{B_{i,max}[n]}h_p P_i} = 23.52$ spikes in all pre-synaptic terminals is needed to generate a spike in post-synaptic neuron. Moreover, the average number of spikes arrive to all pre-synaptic terminals is $\mu_{st} = M(1 - \exp(-\lambda\Delta t))$ according to (11). Hence, the probability of spike generation in post-synaptic terminal tends to zero for $M \leq 23$ independent from the activation of pre-synaptic terminals, thus, the mutual information between input and output of the channel is negligible as shown in Fig. 3. However, the chance of arrival of enough spikes for activating post-synaptic terminal increases for higher values of M .

As it is shown in the Fig. 3(a), for $M \in [30, 50, 70, 100]$, increasing λ first improves the mutual information between input and output until reaching its maximum value. Then, further increase in λ decreases the mutual information. The reasons of this trend is investigated in the following.

- For *small values of λ* , the probability of spike arrival in each pre-synaptic terminal during a time step, i.e., $P\{S_i[n] = 1\} = 1 - \exp(-\lambda\Delta t)$, is very small. Thus, the total number of spikes arrived in all pre-synaptic input is insufficient to fire a spike in post-synaptic neuron. Hence, if λ is small, the probability of spike generation in post-synaptic terminal, thus, the mutual information between input and output of the channel, tends to zero.
- For *very big values of λ* , the probability of spike arrival in each pre-synaptic terminal tends to 1. Thus, if the number of input neurons, M , is high enough, there is sufficient number of spikes in all pre-synaptic inputs to generate a spike in post-synaptic terminal during all time steps. Hence, the mutual information between input and output of the channel tends to zero.
- *Increasing spiking rate, λ* , monotonically increases the probability of spike arrival in i th pre-synaptic terminal, which in turn increases the number of all spikes arrived in all pre-synaptic neurons. Hence, the probability of spike generation in post-synaptic terminal, i.e., $P\{Y[n] = 1\}$ monotonically increases from 0 in low values of λ to 1 in higher values of λ . Note that, the maximum mutual

information happens when $P\{Y[n] = 1\}$ reaches an optimum value. Moreover, I becomes less than its maximum value for pre-synaptic activities causing higher or lower $P\{Y[n] = 1\}$ compared to its optimum value. Hence, increase in spiking rate, λ , increases the mutual information, I , until reaching its maximum value as shown in Fig. 3(a). However, after reaching the maximum mutual information, increasing λ decreases I since it causes more deviation from optimum value of $P\{Y[n] = 1\}$.

Moreover, since the average number of spikes arrive to all pre-synaptic terminals is $\mu_{st} = M(1 - \exp(-\lambda\Delta t))$, the maximum mutual information can be achieved with lower value of M if λ is increased.

As it is shown in Fig. 3(a), the changes in mutual information with respect to λ is faster for higher values of M . This makes the performance of the system sensitive to jitters in λ for higher values of M , which should be considered in future applications of this communication paradigm.

The average consumed metabolic energy, w_p , for different spiking rates, λ , and number of input neurons, M , is shown in Fig. 3(b). Either increasing λ or M increases the number of spikes at the input, which in turn increases the average required metabolic energy, w_p , based on (5). Moreover, the metabolic energy required to maintain resting potential also increases for higher values of M .

B. Performance for Different Number of Pre-synaptic Inputs

The sum rate of the MISO channel without considering the metabolic cost constraint is calculated by maximizing the mutual information, shown in Fig. 3(a), over λ . As depicted in Fig. 3(c), higher number of pre-synaptic terminals, M , increases the maximum achievable sum rate, i.e., C , since the average and standard deviation of number of spikes in the input increases. However, the increase rate of C is decreasing by increasing M . This should be considered in design of nanoscale communication systems based on neuro-spike communication since increasing number of inputs does not efficiently improve the achievable sum rate of the system.

C. Maximum Achievable Sum Rate Versus Metabolic Cost

Limiting the average metabolic energy available for this MISO communication, i.e., W , controls the average number of pre-synaptic terminals that can have a spike in a given

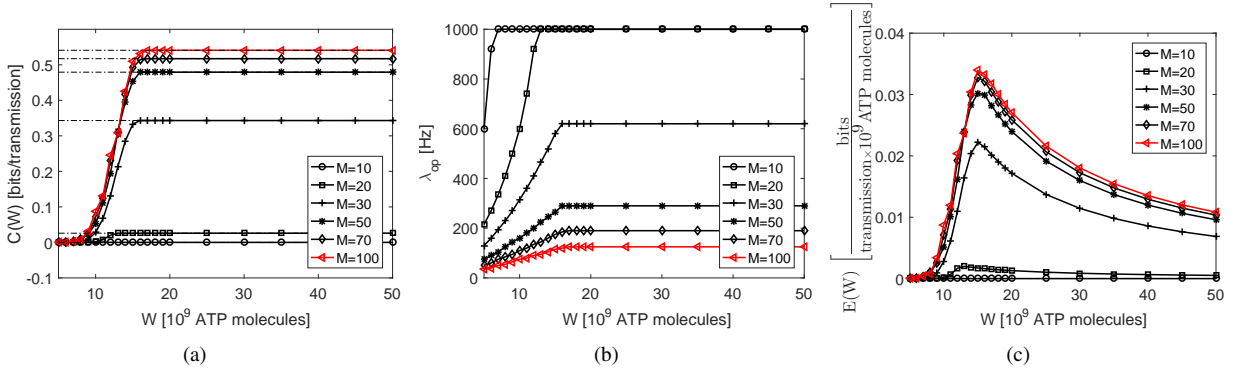


Fig. 4. (a) Sum rate of MISO synaptic channel with metabolic cost constraint (b) the spiking rate that maximizes the sum rate, i.e., λ_{op} and (c) the maximum achievable sum rate per unit metabolic energy.

time step. Hence, it affects the maximum achievable mutual information. The maximum achievable sum rate of the MISO channel as a function of W is shown in Fig. 4(a) for different number of pre-synaptic neurons. The dotted lines in this figure show the sum rate that can be achieved for a particular number of inputs in the absence of metabolic cost constraint.

By increasing W more number of spikes are allowed in the input, which increases the mutual information as observed in Fig. 3(a). Hence, relaxing the upper bound on the average consumed metabolic energy increases the maximum achievable sum rate of the channel, $C(W)$, as it is shown in Fig. 4(a). Moreover, $C(W)$ increases with almost the same rate for each M since it is a function of average number of spikes allowed at the input, which is not affected by changing M for a constant W . As it is shown in Fig. 4(a), $C(W)$ is saturating after reaching the peak of mutual information for each value of M . Furthermore, this peak is occurring at almost the same value of W for all M since it depends on number of pre-synaptic input and the required metabolic energy for spike generation is very higher than the required energy for achieving resting potential in neurons. However, it can be observed that as number of pre-synaptic inputs increases a slightly higher W is required to achieve the peak of mutual information.

The average number of spikes in the input of the MISO neuro-spike communication is limited by the metabolic cost constraint, i.e., $w_p < W$. Hence, possible values of spiking rate, λ , that can be used to calculate the maximum achievable sum rate in (6) is changing for different values of W . Values of spiking threshold that maximizes the the sum rate, i.e., λ_{op} , are shown in Fig. 4(b) for different values of W . Since increasing W allows bigger values of λ to be used in (6), we can observe that higher λ_{op} is obtained for bigger values of W for each M . It is also shown in Fig. 4(b) that λ_{op} saturates at the value corresponding to the peak of mutual information in Fig. 3(a). Moreover, the maximum sum rate is achieved at lower λ_{op} for higher values of M since average number of spikes at the input increases with increasing M for a certain value of λ .

D. Information-Cost Efficiency

The amount of consumed metabolic energy is an important factor in determining the rate of error free information transmission between brain and the outside world. As shown in

Fig. 4(a), the sum rate of MISO neuro-spike communication increases with increasing W until reaching a saturation point. After this point, providing more metabolic energy does not improve the achievable sum rate. Hence, we find a trade-off in terms of information-cost efficiency, $E(W) = \frac{C(W)}{W}$, as shown in Fig. 4(c). The parameter $E(W)$, showing the maximum achievable sum rate per unit metabolic energy, can be used to select the optimum value of W in designing a MISO neuro-spike communication system. It can be observed that if enough metabolic energy is not provided for the system, the number of active inputs are decreased, thus reducing the maximum achievable sum rate. Moreover, increasing the available metabolic energy after reaching the peak of $E(W)$ does not improve the performance of the system.

E. Impacts of Spike Generation Thresholds on Sum Rate

The spike generation threshold changes according to the memory of postsynaptic neuron [23], which can affect the information transmission over the MISO neuro-spike communication channel. Here, we utilize the closed form equation derived for the sum rate of the MISO synaptic channel with constant spiking threshold in Section III, and find the impact of variations in the spiking threshold on the performance of the channel. As depicted in Fig. 5(a), more metabolic energy is required to reach the peak of $C(W)$ by increasing the spiking threshold, θ , since more number of spikes are required in the input for spike generation at output neuron. Moreover, the peak of $C(W)$ decreases with increasing spiking threshold, θ_0 , when M is constant as shown in Fig. 5(a), which is the same as observations in Fig. 3(c). The reason is that changes in $\theta_0 - E(t)$, which is important in deriving the probability of spike generation at output neuron, is the same for (i) increasing spiking threshold θ_0 when number of input neurons is constant, considered in Fig. 5(a), and (ii) decreasing number of input neurons M , which leads to smaller $E(t)$, when spiking threshold, θ_0 , is constant, studied in Fig. 3(c).

F. Sum Rate vs Number of Released Neurotransmitters

One of the important factors for the performance of neuro-spike communication channel is the number of neurotransmitters in each vesicle, which can be different from

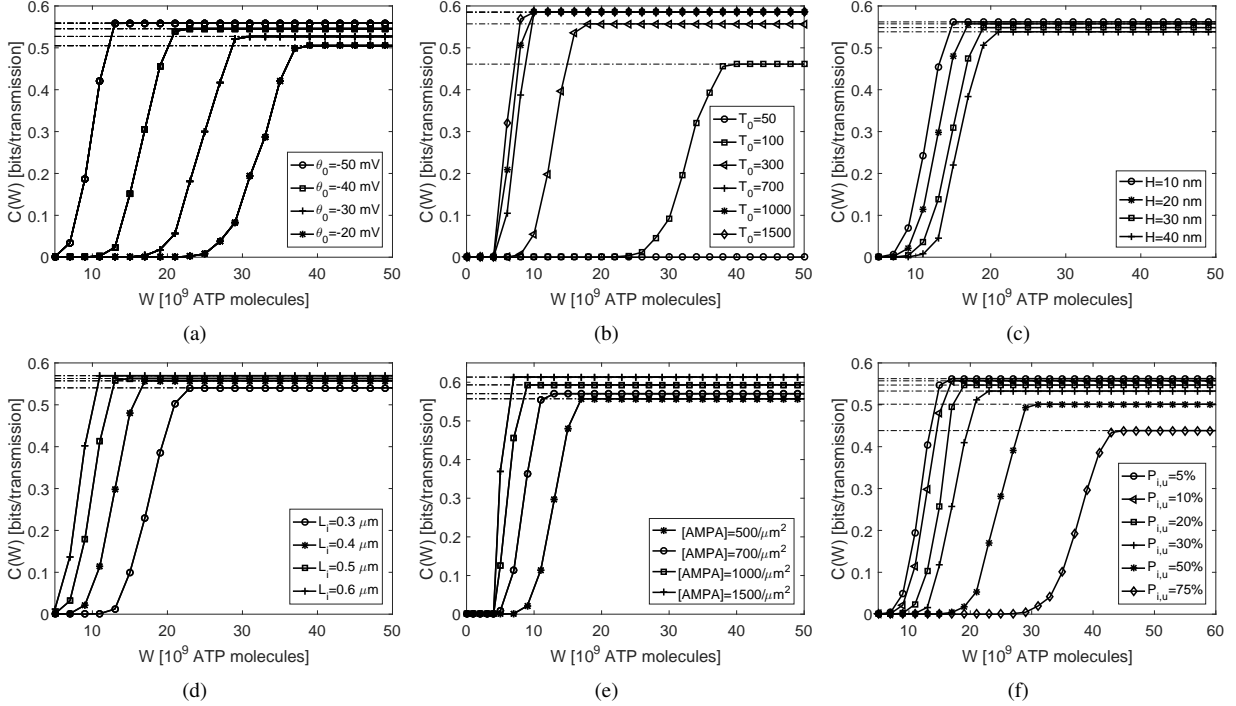


Fig. 5. Sum rate of MISO synaptic channel with metabolic cost constraint considering $M = 150$ and different (a) spiking thresholds, (b) number of released neurotransmitter, (c) synaptic cleft heights, (d) synaptic cleft side lengths, (e) density of receptors, (f) uptake probabilities.

one neuron to another one and can also be affected by different diseases such as Parkinson [31]. Here, we analyze how changes in number of neurotransmitters in a vesicle, T_0 , affects the performance of MISO neuro-spike communication channel. By increasing T_0 , number of bound neurotransmitters per vesicle release increases which results in higher amplitude of EPSP per synapse. This scenario is equivalent with increasing M when T_0 is fix, for which changes in sum rate is shown in Fig. 3(c). Hence, the peak of $C(W)$ is higher for bigger values of T_0 as shown in Fig. 5(b). Furthermore, bigger values of EPSP per synapse results in need for less number of pre-synaptic spikes to fire a spike at output neuron. Hence, the peak of $C(W)$ is reached with consuming lower metabolic energy. Moreover, changes in $C(W)$ caused by increasing T_0 saturate since the available number of receptors in postsynaptic neuron is limited and almost all of them are bound to a neurotransmitter in the saturation point. Hence, further increase of T_0 does not affect the EPSP generation and the performance of this channel.

G. Sum Rate for Different Synaptic Geometries

Synaptic geometries strongly affect the number of neurotransmitters that bind to receptors of since by increasing either the height or the length of the synapse, the distance that neurotransmitters need to pave to reach receptors increases. This increases the chance of diffusion of neurotransmitters to outside of synaptic cleft or re-uptake of them by pre-synaptic terminal, which results in reduction of the amplitude of EPSP generated per vesicle release. Hence, more number of pre-synaptic spikes, thus, more metabolic energy, is required for

spike generation. As a result, peak of $C(W)$ occurs at higher values of W as shown in Fig. 5(c) and Fig. 5(d).

H. Sum Rate vs Density of Post-synaptic Receptors

Increasing the density of post-synaptic receptors, increases the number of bound neurotransmitters, thus, the peak of EPSP generated, per vesicle release. These consequences are the same with the outcomes of increasing number of neurotransmitters per vesicle when the density of receptors is constant as discussed in Section IV-F. Hence, increasing the receptors density results in bigger peak of $C(W)$ and the occurrence of peak at lower W as shown in Fig. 5(e). Moreover, the amount of changes in $C(W)$ reduces by increasing density of receptors since after some point the released neurotransmitters are not enough for binding to the newly added receptors.

I. Sum Rate vs Clearance of Neurotransmitters from Synapse

In this section, we study the impact of changes in the probability of uptake of neuro-transmitters by pre-synaptic neurons, $P_{i,u}$, on the performance of MISO neuro spike communication. Increasing $P_{i,u}$ reduces number of bound neurotransmitters to receptors of post-synaptic neuron, thus, decreases the amplitude of EPSP generated, per vesicle release. These consequences are the same with the outcomes of decreasing number of neurotransmitters per vesicle when $P_{i,u}$ is constant as discussed in Section IV-F. Hence, increasing $P_{i,u}$ results in smaller peak of $C(W)$ and the occurrence of peak at higher W as shown in Fig. 5(f).

V. CONCLUSION

Certain limitations and constraints exist on the transmission capacity of a MISO neuro-spike communication system as a result of different stochastic processes involved in it and the available metabolic energy for neurons to carry out their routine processing. In this paper, we derived the closed form equation for the mutual information between input and output of a MISO neuro-spike communication system. Moreover, we quantified the maximum rate of information transmission after taking into account the consumed metabolic energy in terms of ATP molecules. Furthermore, we have studied impacts of number of pre-synaptic terminals, biological parameters of the channel and available metabolic energy on the maximum achievable sum rate of the MISO neuro-spike communication. The results provided in this paper gives insights on (i) selecting channel parameters while designing bio-inspired nanonetworks based on neuro-spike communication and (ii) the impact of diseases that change the neuro-spike communication channel characteristics on the performance of nervous nanonetwork.

REFERENCES

- [1] O. B. Akan, H. Ramezani, T. Khan, N. A. Abbasi, and M. Kescu, "Fundamentals of molecular information and communication science," *Proc. IEEE*, vol. 105, no. 2, pp. 306–318, 2017.
- [2] E. Balevi and O. B. Akan, "A physical channel model for nanoscale neuro-spike communications," *IEEE Trans. Comm.*, vol. 61, no. 3, pp. 1178–1187, 2013.
- [3] L. Galluccio, S. Palazzo, and G. E. Santagati, "Characterization of molecular communications among implantable biomedical neuro-inspired nanodevices," *Nano Commun. Netw.*, vol. 4, no. 2, pp. 53–64, 2013.
- [4] A. Manwani and C. Koch, "Detecting and estimating signals over noisy and unreliable synapses: information-theoretic analysis," *Neural computation*, vol. 13, no. 1, pp. 1–33, 2001.
- [5] H. Ramezani, C. Koca, and O. B. Akan, "Rate region analysis of multi-terminal neuronal nanoscale molecular communication channel," in *Proc. 17th IEEE-NANO Conf.* IEEE, 2017, pp. 59–64.
- [6] M. Veletić, P. A. Floor, Y. Chahibi, and I. Balasingham, "On the upper bound of the information capacity in neuronal synapses," *IEEE Trans. Commun.*, vol. 64, no. 12, pp. 5025–5036, 2016.
- [7] D. Malak and O. B. Akan, "A communication theoretical analysis of synaptic multiple-access channel in hippocampal-cortical neurons," *IEEE Trans. Commun.*, vol. 61, no. 6, pp. 2457–2467, 2013.
- [8] H. Ramezani and O. B. Akan, "Information capacity of vesicle release in neuro-spike communication," *IEEE Commun. Lett.*, vol. 22, no. 1, pp. 41–44, 2018.
- [9] H. Ramezani, T. Khan, and O. B. Akan, "Information theoretical analysis of synaptic communication for nanonetworks," in *Proc. 37th IEEE INFOCOM.* IEEE, 2018.
- [10] M. F. Bear, B. W. Connors, and M. A. Paradiso, *Neuroscience: Exploring the Brain*, 3rd ed. Lippincott Williams & Wilkins, 2007.
- [11] B. Sengupta and M. B. Stemmler, "Power consumption during neuronal computation," *Proc. IEEE*, vol. 102, no. 5, pp. 738–750, 2014.
- [12] J. J. Harris, R. Jolivet, E. Engl, and D. Attwell, "Energy-efficient information transfer by visual pathway synapses," *Current Biology*, vol. 25, no. 24, pp. 3151–3160, 2015.
- [13] L. Kostal and R. Kobayashi, "Optimal decoding and information transmission in hodgkin-huxley neurons under metabolic cost constraints," *Biosys.*, vol. 136, pp. 3–10, 2015.
- [14] L. Kostal, P. Lansky, and M. D. McDonnell, "Metabolic cost of neuronal information in an empirical stimulus-response model," *Biological cybernetics*, vol. 107, no. 3, pp. 355–365, 2013.
- [15] J. R. Geiger and P. Jonas, "Dynamic control of presynaptic Ca^{2+} inflow by fast-inactivating K^{+} channels in hippocampal mossy fiber boutons," *Neuron*, vol. 28, no. 3, pp. 927–939, 2000.
- [16] H. Ramezani and O. B. Akan, "A communication theoretical modeling of axonal propagation in hippocampal pyramidal neurons," *IEEE Trans. NanoBiosci.*, vol. 16, no. 4, pp. 248–256, 2017.
- [17] M. Veletić, P. A. Floor, Z. Babić, and I. Balasingham, "Peer-to-peer communication in neuronal nano-network," *IEEE Trans. Commun.*, vol. 64, no. 3, pp. 1153–1166, 2016.
- [18] L. E. Dobrunz and C. F. Stevens, "Heterogeneity of release probability, facilitation, and depletion at central synapses," *Neuron*, vol. 18, no. 6, pp. 995–1008, 1997.
- [19] V. N. Murthy and C. F. Stevens, "Reversal of synaptic vesicle docking at central synapses," *Nature neuroscience*, vol. 2, pp. 503–507, 1999.
- [20] T. Khan, B. A. Bilgin, and O. B. Akan, "Diffusion-based model for synaptic molecular communication channel," *IEEE Trans. NanoBiosci.*, 2017.
- [21] A. Destexhe, Z. Mainen, and T. Sejnowski, "kinetic models for synaptic interactions," *The Handbook of Brain Theory and Neural Networks*, pp. 1126–1130, 2002.
- [22] M. Fernandez and S. Williams, "Closed-form expression for the poisson-binomial probability density function," *IEEE Trans. Aerospace and Electronic Systems*, vol. 46, no. 2, pp. 803–817, April 2010.
- [23] R. Kobayashi, Y. Tsubo, and S. Shinomoto, "Made-to-order spiking neuron model equipped with a multi-timescale adaptive threshold," *Frontiers in computational neuroscience*, vol. 3, p. 9, 2009.
- [24] D. Attwell and S. B. Laughlin, "An energy budget for signaling in the grey matter of the brain," *J. Cerebral Blood Flow & Metabolism*, vol. 21, no. 10, pp. 1133–1145, 2001.
- [25] T. Schikorski and C. F. Stevens, "Quantitative ultrastructural analysis of hippocampal excitatory synapses," *J. Neurosci.*, vol. 17, no. 15, pp. 5858–5867, 1997.
- [26] R. Plonsey and R. C. Barr, *Bioelectricity: a quantitative approach.* Springer, 2007.
- [27] L. P. Savtchenko and D. A. Rusakov, "The optimal height of the synaptic cleft," *Proc Natl Acad Sci U S A*, vol. 104, no. 6, pp. 1823–1828, 2007.
- [28] T. A. Nielsen, D. A. DiGregorio, and R. A. Silver, "Modulation of glutamate mobility reveals the mechanism underlying slow-rising ampa epscs and the diffusion coefficient in the synaptic cleft," *Neuron*, vol. 42, no. 5, pp. 757–771, 2004.
- [29] J. Montes, J. M. Peña, J. DeFelipe, O. Herreras, and A. Merchan-Perez, "The influence of synaptic size on ampa receptor activation: A monte carlo model," *PLoS one*, vol. 10, no. 6, p. e0130924, 2015.
- [30] N. Agmon and A. L. Edelman, "Collective binding properties of receptor arrays," *Biophys. J.*, vol. 72, no. 4, p. 1582, 1997.
- [31] O. Hornykiewicz, "Biochemical aspects of parkinson's disease," *Neurology*, vol. 51, no. 2 Suppl 2, pp. S2–S9, 1998.